Acta Radiologica Open
5(8) 1–6

DOI: 10.1177/2058460116649799
arr.sagepub.com
SAGE

Sclerosing angiomatoid nodular transformation (SANT) of the spleen: a case report with FDG-PET findings and literature review

Yumi Imamura[1], Reiko Nakajima[1], Kazuha Hatta[2], Akiyoshi Seshimo[2], Tatsuo Sawada[3], Koichiro Abe[1] and Shuji Sakai[1]

Abstract

We report the 18F-fluorodeoxyglucose (FDG) positron emission tomography (PET)/computed tomography (CT) findings of sclerosing angiomatoid nodular transformation (SANT) of the spleen. The patient was a 37-year-old woman with a splenic mass incidentally found on abdominal ultrasound. FDG-PET/CT showed weak FDG accumulation (maximum standardized uptake value = 3.65). An unenhanced CT scan showed a low density and well-circumscribed splenic tumor that demonstrated weak enhancement from the arterial to delayed phase. Although hemangioma or hamartoma of the spleen was preoperatively diagnosed, histopathological examination revealed SANT. Therefore, when a splenic tumor with weak contrast medium enhancement and low FDG accumulation is observed, SANT should be considered as a differential diagnosis. Although CT and magnetic resonance imaging features of SANT have been reported, there are few reports on FDG-PET/CT findings. We report the radiological features of SANT, including FDG-PET/CT, and review the literature on SANT.

Keywords

Sclerosing angiomatoid nodular transformation (SANT), spleen, 18F-fluorodeoxyglucose (FDG) positron emission tomography (PET), computed tomography (CT)

Date received: 25 March 2016; accepted: 22 April 2016

Introduction

Sclerosing angiomatoid nodular transformation (SANT) of the spleen is a rare, benign vascular tumor (1). Although computed tomography (CT) imaging and magnetic resonance imaging (MRI) features of SANT have been reported (2–5), we found only 10 cases in the English literature (6–12) of 18F-fluorodeoxyglucose (FDG) positron emission tomography (PET)/CT findings. Here we report CT, MRI, and PET findings of a case of SANT.

Case report

Abdominal ultrasonography (US) of a 37-year-old woman during a routine health examination incidentally revealed a 5-cm hypoechoic mass in the spleen. She underwent contrast-enhanced CT and MRI at a local hospital. She then presented to our hospital for further diagnostic workup and possible treatment of a suspected splenic benign vascular tumor. FDG-PET/

[1]Department of Diagnostic Imaging and Nuclear Medicine, Tokyo Women's Medical University, Tokyo, Japan
[2]Department of Surgery II, Tokyo Women's Medical University, Tokyo, Japan
[3]Department of Pathology, Tokyo Women's Medical University, Tokyo, Japan

Corresponding author:
Reiko Nakajima, Department of Diagnostic Imaging and Nuclear Medicine, Tokyo Women's Medical University, 8-1 Kawada-cho, Shinjuku-ku, Tokyo 162-8666, Japan.
Email: nakajima.reiko@twmu.ac.jp

CT was performed to determine if the mass was a hemangioma, hamartoma, or a malignant lymphoma of the spleen, as initially suspected. A maximum intensity projection (MIP) image showed a weak FDG uptake in the tumor (Fig. 1a). FDG accumulation in the tumor was low and heterogeneous with a maximum standardized uptake value (SUVmax) of 3.65 (Fig. 1b and c). No abnormal FDG accumulation was found elsewhere in the body. Considering these findings, a splenic benign vascular tumor was suspected; thus, we decided to perform a follow-up examination.

After 8 months, dynamic CT was performed. CT images revealed a low-attenuation, well-circumscribed splenic tumor (Fig. 2a) measuring 4.5×5 cm, with peripheral enhancements on the arterial phase image (Fig. 2b) and heterogeneous enhancements on the portal venous and delayed phase images (Fig. 2c and d). The delayed phase images showed that the lesion was progressively enhancing toward the center, and the central "scar" remained visible (Fig. 2d). MRI was simultaneously performed, which showed predominantly decreased signaling on T1-weighted (T1W) and T2-weighted (T2W) images with small areas of hyperintensity on both sequences (Fig. 3a and b). A diffusion-weighted image also showed hypointensity of the mass (Fig. 3c). Following intravenous administration of gadolinium contrast medium (gadopentetate dimeglumine, Magnevist, Bayer, Osaka, Japan), peripheral enhancement and delayed central filling of the lesion was seen with a persistent non-enhancing central hypointense focus (Fig. 3d–f). Although follow-up radiological images showed no changes in tumor characteristics or size and with a preoperative diagnosis of a benign vascular tumor, laparoscopic splenectomy was performed.

The gross splenectomy specimen was a well-circumscribed 4.5×4 cm mass weighing 280 g, which was found in the anterior, upper portion of the spleen. The cut surface of the tumor was white (Fig. 4a).

Microscopically, the tumor was composed of multiple angiomatoid nodules separated by fibrosclerotic stroma. Inflammatory cells and extravasated red blood cells were observed in the angiomatoid nodules. The fibrosclerotic stroma contained many immature myofibroblasts (Fig. 4b). Immunohistochemically, the tumor cells were positive for CD34, CD8, and CD31

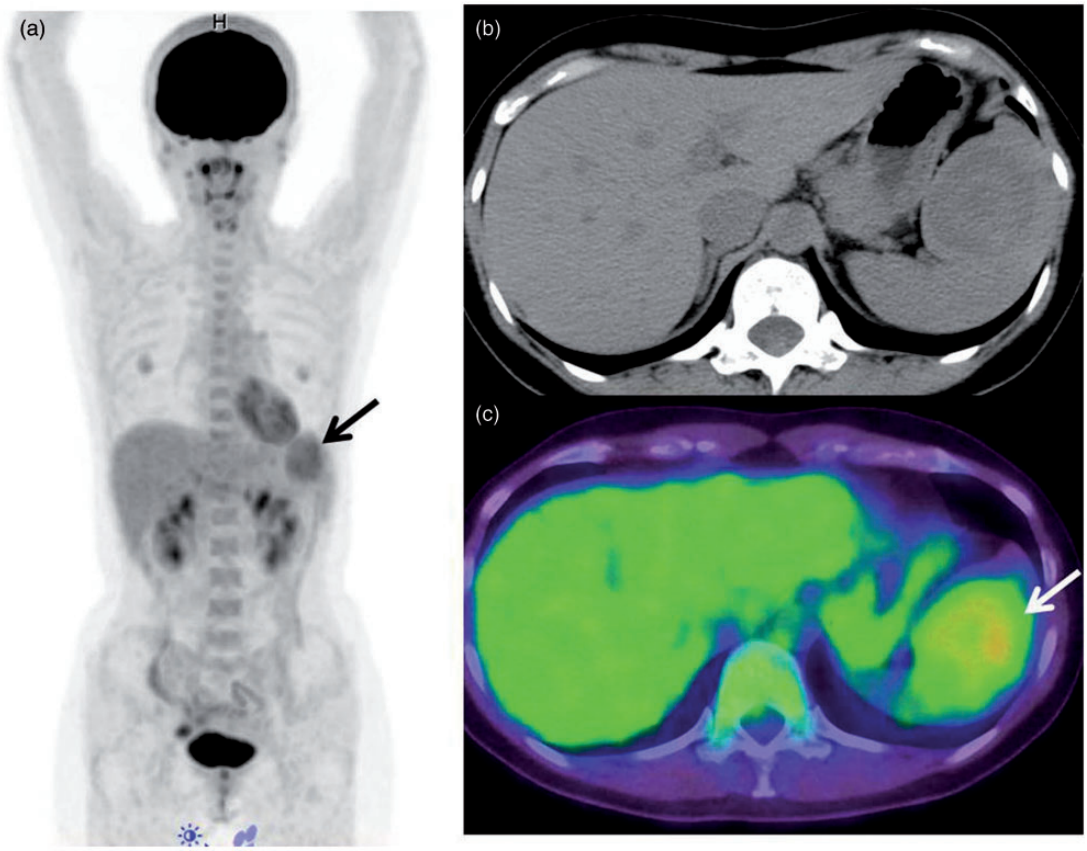

Fig. 1. Low FDG accumulation in the splenic tumor on maximal intensity projection and (b) axial CT and (c) PET/CT images. The SUVmax value of the tumor was 3.65 (a, c, arrows).

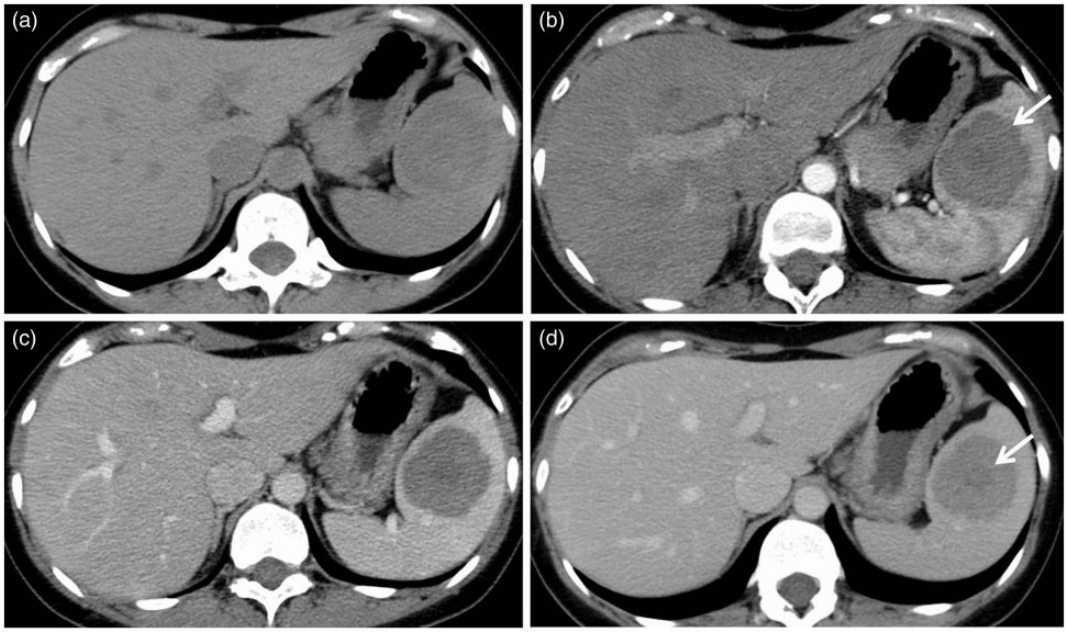

Fig. 2. At 8-month follow-up. (a) Axial unenhanced, (b) arterial phase, (c) portal venous phase, and (d) delayed enhanced imaging of the abdomen show that (a) the splenic lesion is initially mildly hypodense compared with the normal spleen. (b) Arterial phase imaging shows marked enhancement of the periphery of the lesion with a few faintly visible septae (arrow) penetrating the center of the lesion from the periphery. (c) The portal venous phase image again shows the hypervascular rim of the lesion. (d) Delayed enhanced imaging shows that the lesion became progressively enhanced toward its center. However, the central "scar" remained visible (arrow).

(Fig. 4 c–e), weakly positive for α-smooth muscle-specific actin and CD68 (Fig. 4 f), and negative for cytokeratin and immunoglobulin G4 in angiomatoid nodules. Therefore, we diagnosed the mass as SANT. The patient is currently disease-free after 12 months of follow-up.

Discussion

SANT of the spleen was recognized as a district pathological entity in 2004 by Martel et al. (1). Macroscopically, SANT is a well-demarcated solitary mass composed of dense fibrous stroma containing reddish-brown nodules. The most distinctive microscopic findings are multiple angiomatoid nodules separated by collagenous bundles (1). Immunohistochemically, theses nodules are composed of three types of blood vessels: the cord capillary type, CD31+/CD34+/CD8–; the sinusoid type, CD31+/CD34–/CD8+; and the small vein type, CD31+/CD34–/CD8– (1). The distinctive histological appearance of SANT should allow differentiation from a hemangioma. There is a slight female predominance, with a male:female ratio of 1:1.4, and most patients are middle-aged (1,4). SANT is a rare, benign vascular tumor of the spleen, with only approximately 100 cases reported thus far, predominantly in the pathology literature (2–5). Although there are reports on the radiological findings of SANTs using CT and MRI, only 10 case reports are available in the English literature (6–12) on the evaluation of SANTs using FDG-PET. Lee et al. (6) were the first to describe the appearance of SANT on FDG-PET. Kim et al. (10) described the FDG accumulation of SANT in three patients in 2012, whereas our report describes 11 cases, including our case on SANTs; to the best of our knowledge, this is the largest number of FDG PET findings reported for SANT in the literature. Based on these cases, the findings for the FDG uptake of SANT on PET can be considered to provide an accurate diagnosis. The findings of the 10 previously described case reports on SANTs and the present case are summarized in Table 1. Of these 11 SANTs, 10 showed FDG accumulations and one did not. FDG accumulation was not very high, with a median (± standard deviation) SUVmax of 2.8 ± 1.20 (range, 2.0–5.4). The previous cases and our case had an FDG accumulation range similar to that reported by Kim et al. (10). Accordingly, an awareness of the FDG PET/CT findings of SANT and recognition of the accumulation ranges may aid in differential diagnosis. FDG accumulation patterns were heterogeneous in six cases and nodular, peripheral, and homogenous in one case each. According to Feng et al. (11), the nodular accumulation in the MIP images appeared as "prunes on bread," where "prunes" represent angiomatoid nodules with FDG uptake and "bread" represents splenic tissue. The abundance of cells, including hemosiderin-laden

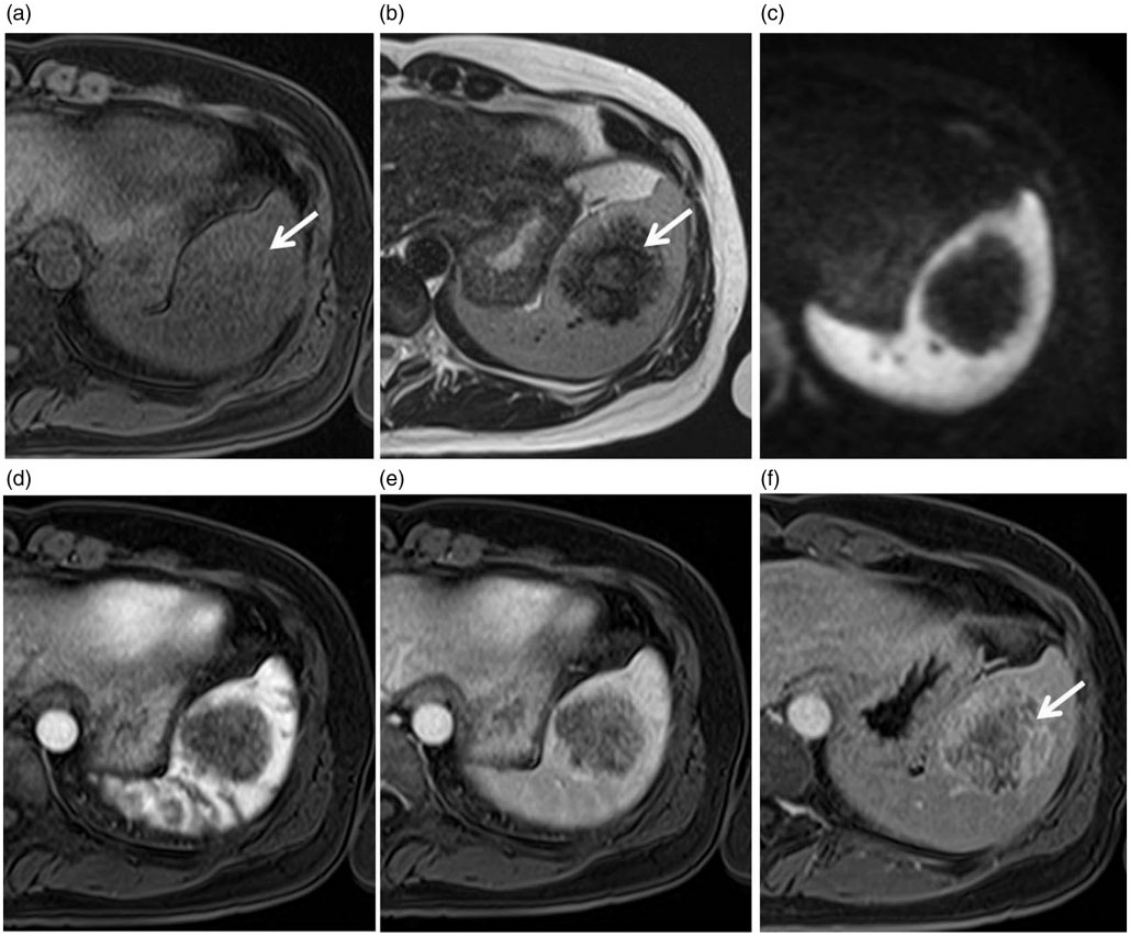

Fig. 3. At 8-month follow-up. (a) T1W and (b) T2W MR images showing a lesion that is hypointense to the splenic parenchyma with a central increasingly hyperintense stellate focus (arrows). (c) Diffusion-weighted image showing also hypointense. MR images following the administration of an intravenous contrast medium. (d) Arterial phase post-contrast enhanced T1W, fat-saturated MR image showing early peripheral enhancement. (e) Portal phase showing centripetal filling. (f) Delayed phase showing progressive centripetal filling, with a persistent non-enhancing central hypointense focus (arrow).

macrophages, myofibroblasts, lymphocytes, and plasma cells, may explain the FDG uptake in splenic SANTs because the degree of FDG accumulation reflects the number of these cells in the tumor.

In our patient, FDG accumulation in the tumor was low and heterogeneous, with a SUVmax of 3.65, similar to that in previous reports (6–12). The low degree of FDG accumulation is reflected by the number of inflammatory cells and hemosiderin-laden macrophages in angiomatoid nodules. In fact, the mass in the present case was weakly positive for CD68 (Fig. 4f), a marker of histiocytes.

The differential diagnosis includes other benign lesions, such as hamartomas, hemangiomas, hemangioendotheliomas, littoral cell angiomas, inflammatory myofibroblastic lesions, malignant lesions, such as metastatic tumors, angiosarcomas, and lymphoma. In general, FDG uptake is high in malignant tumors and inflammatory myofibroblastic lesions; thus, the degree of FDG accumulation can be used to differentiate SANT from other malignant tumors. However, SANT cannot be easily distinguished from other benign splenic tumors based on FDG-PET/CT findings only.

Tissue samples can be obtained by either splenectomy or percutaneous biopsy. Most previous cases of SANT were diagnosed by splenectomy. The diagnosis of SANT may be established by percutaneous biopsy; however, due to the potential for an increased rate of complications associated with percutaneous biopsy of vascular lesions of the spleen and concerns regarding the possibility of spontaneous rupture of a large vascular splenic lesion, splenectomy is often the modality of choice for diagnosis and management of SANT of the spleen. However, Gutzeit et al. (13) reported the use of ultrasound-guided core needle biopsy for the diagnosis of SANT, although greater caution is required because

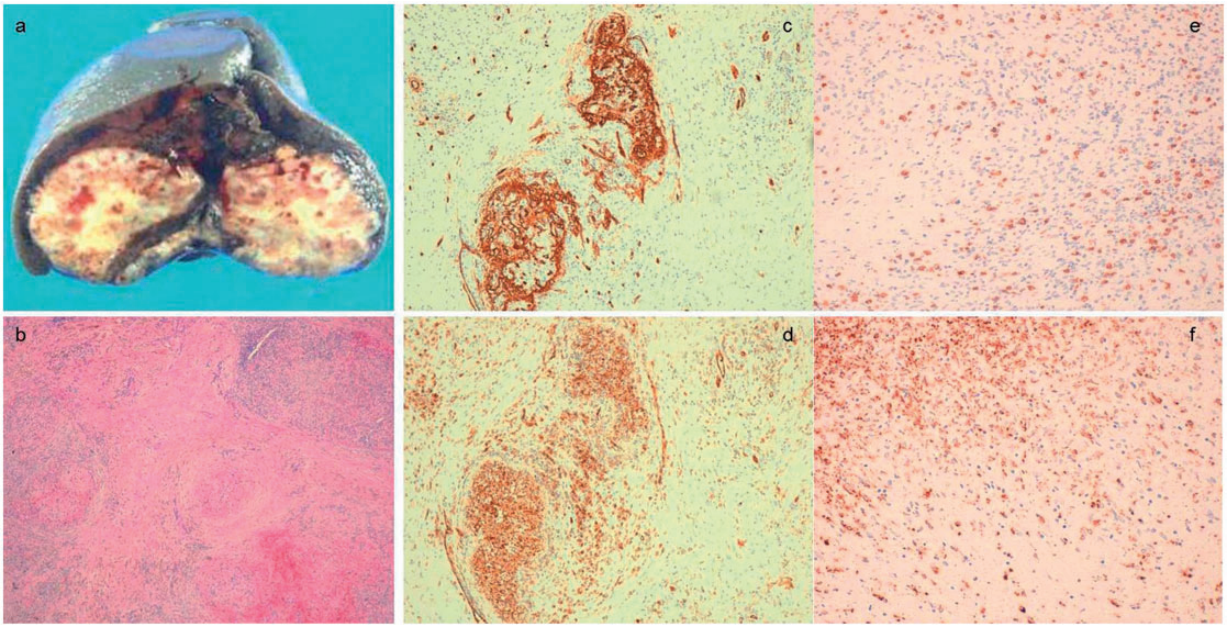

Fig. 4. (a) The cut surface of the tumor (4.5 × 4 cm) is shown. The main part of the tumor was white. The splenic lesion consisted of multiple angiomatoid nodules surrounded by variable fibrous bands (b, H&E, original magnification × 4). Immunostaining for CD34 (c, original magnification × 10), CD31 (d, original magnification × 10), and CD8 (e, original magnification × 20) is shown. Selective staining of narrow capillaries in the angiomatoid nodules is shown. Immunohistochemically, the tumor cells were weakly positive for CD68 (f, original magnification × 20).

Table 1. Summary of the 18F-FDG/PET findings of SANT in previous reports.

Author (reference number)	Age (years)/Sex	Diameter (mm)	SUVmax	FDG accumulation pattern	Diagnosis
Lee et al. (6)	58/M	42	Not referred	Heterogeneous	Splenectomy
Koreishi et al. (7)	58/F	40	4.7	Not referred	Splenectomy
	64/F	15	No significant accumulation		
Subhawong et al. (8)	27/F	102	2.2	Homogenous	Splenectomy
Thacker et al. (9)	80/M	90	4.5	Heterogeneous	Splenectomy
Kim et al. (10)	39/M	47	2.7	Heterogeneous	Splenectomy
	39/M	45	2.8	Heterogeneous	Splenectomy
	50/M	28	2.0	Heterogeneous	Splenectomy
Feng et al. (11)	44/F	60	2.8	Nodular	Splenectomy
Lapa et al. (12)	51/M	80	5.4	Peripheral	Splenectomy
Present case	37/F	45	3.65	Heterogeneous	Splenectomy

of the higher incidence of complications associated with percutaneous biopsy of vascular spleen lesions. A meta-analysis by McInnes et al. (14) reported a major complication rate of 2.2% for biopsies performed with an ≤ 18-gauge needle, which is similar to that reported for biopsies of the liver and kidney. Moreover, image-guided percutaneous biopsy demonstrated a high degree of diagnostic accuracy (sensitivity, 87.0%; specificity, 96.4%).

SANT is benign with no recurrence or malignant alteration in cases reported thus far. Image-guided biopsy might be a potential diagnostic option.

In conclusion, we report a case of a SANT of the spleen and its features on FDG-PET/CT. When a patient presents with a splenic tumor with low FDG accumulation, SANT should be considered in addition to other vascular tumors. Familiarity with cross-sectional imaging findings will help the clinician to make an accurate diagnosis.

Declaration of conflicting interests

The author(s) declared no potential conflicts of interest with respect to the research, authorship, and/or publication of this article.

Funding

The author(s) received no financial support for the research, authorship, and/or publication of this article.

References

1. Martel M, Cheuk W, Lombardi L, et al. Sclerosing angiomatoid nodular transformation (SANT): report of 25 cases of a distinctive benign splenic lesion. Am J Surg Pathol 2004;28:1268–1279.
2. Raman SP, Singhi A, Horton KM, et al. Sclerosing angiomatoid nodular transformation of the spleen (SANT): multimodality imaging appearance of five cases with radiology pathology correlation. Abdom Imaging 2013;38: 827–834.
3. Li L, Fisher DA, Stanek AE. Sclerosing angiomatoid nodular transformation (SANT) of the spleen: addition of a case with focal CD68 staining and distinctive CT features. Am J Surg Pathol 2005;29:839–841.
4. Falk GA, Nooli NP, Morris-Stiff G, et al. Sclerosing angiomatoid nodular transformation (SANT) of the spleen: Case report and review of the literature. Int J Surg Case Rep 2012;3:492–500.
5. Raman SP, Singhi A, Horton KM, et al. Sclerosing angiomatoid nodular transformation of the spleen (SANT): multimodality imaging appearance of five cases with radiology-pathology correlation. Abdom Imaging 2013;38: 827–834.
6. Lee D, Wood B, Formby M, et al. F-18 FDG-avid sclerosing angiomatoid nodular transformation (SANT) of the spleen: case study and literature review. Pathology 2007;39:181–183.
7. Koreishi AF, Saenz AJ, Fleming SE, et al. Sclerosing angiomatoid nodular transformation (SANT) of the spleen: a report of 3 cases. Int J Surg Pathol 2009;17: 384–389.
8. Subhawong TK, Subhawong AP, Kamel I. Sclerosing angiomatoid nodular transformation of the spleen: Multimodality imaging findings and pathologic correlate. J Comput Assist Tomogr 2010;34:206–209.
9. Thacker C, Korn R, Millstine J, et al. Sclerosing angiomatoid nodular transformation of the spleen: CT, MR, PET, and 99 mTc-sulfur colloid SPECT CT findings with gross and histopathological correlation. Abdom Imaging 2010;35:683–689.
10. Kim HJ, Kim KW, Yu ES, et al. Sclerosing angiomatoid nodular transformation of the spleen: clinical and radiologic characteristics. Acta Radiol 2012;53:701–706.
11. Feng YM, Huang YC, Tu CW, et al. Distinctive PET/CT features of splenic SANT. Clin Nucl Med 2013;38: e465–e466.
12. Lapa C, Steger U, Ritter CO, et al. Differentiation of an unclear splenic lesion in a patient with cholangiocarcinoma. Clin Nucl Med 2014;39:470–471.
13. Gutzeit A, Stuckmann G, Dommann-Scherrer C. Sclerosing angiomatoid nodular transformation (SANT) of the spleen: sonographic finding. J Clin Ultrasound 2009;37:308–311.
14. McInnes MD, Kielar AZ, Macdonald DB. Percutaneous image-guided biopsy of the spleen: systematic review and meta-analysis of the complication rate and diagnostic accuracy. Radiology 2011;260:699–708.